Determination of $\mathcal{B}(\chi_{cJ} \to p\bar{p})$ in $\psi(2S)$ decays

J. Z. Bai[1], Y. Ban[10], J. G. Bian[1], X. Cai[1], J. F. Chang[1], H. F. Chen[16], H. S. Chen[1], H. X. Chen[1], J. Chen[1], J. C. Chen[1], Jun. Chen[6], M. L. Chen[1], Y. B. Chen[1], S. P. Chi[1], Y. P. Chu[1], X. Z. Cui[1], H. L. Dai[1], Y. S. Dai[18], Z. Y. Deng[1], L. Y. Dong[1], S. X. Du[1], Z. Z. Du[1], J. Fang[1], S. S. Fang[1], C. D. Fu[1], H. Y. Fu[1], L. P. Fu[6], C. S. Gao[1], M. L. Gao[1], Y. N. Gao[14], M. Y. Gong[1], W. X. Gong[1], S. D. Gu[1], Y. N. Guo[1], Y. Q. Guo[1], Z. J. Guo[15], S. W. Han[1], F. A. Harris[15], J. He[1], K. L. He[1], M. He[11], X. He[1], Y. K. Heng[1], H. M. Hu[1], T. Hu[1], G. S. Huang[1], L. Huang[6], X. P. Huang[1], X. B. Ji[1], Q. Y. Jia[10], C. H. Jiang[1], X. S. Jiang[1], D. P. Jin[1], S. Jin[1], Y. Jin[1], Y. F. Lai[1], F. Li[1], G. Li[1], H. H. Li[1], J. Li[1], J. C. Li[1], Q. J. Li[1], R. B. Li[1], R. Y. Li[1], S. M. Li[1], W. Li[1], W. G. Li[1], X. L. Li[7], X. Q. Li[7], X. S. Li[14], Y. F. Liang[13], H. B. Liao[5], C. X. Liu[1], Fang Liu[16], F. Liu[5], H. M. Liu[1], J. B. Liu[1], J. P. Liu[17], R. G. Liu[1], Y. Liu[1], Z. A. Liu[1], Z. X. Liu[1], G. R. Lu[4], F. Lu[1], J. G. Lu[1], C. L. Luo[8], X. L. Luo[1], F. C. Ma[7], J. M. Ma[1], L. L. Ma[11], X. Y. Ma[1], Z. P. Mao[1], X. C. Meng[1], X. H. Mo[1], J. Nie[1], Z. D. Nie[1], S. L. Olsen[15], H. P. Peng[16], N. D. Qi[1], C. D. Qian[12], H. Qin[8], J. F. Qiu[1], Z. Y. Ren[1], G. Rong[1], L. Y. Shan[1], L. Shang[1], D. L. Shen[1], X. Y. Shen[1], H. Y. Sheng[1], F. Shi[1], X. Shi[10], L. W. Song[1], H. S. Sun[1], S. S. Sun[16], Y. Z. Sun[1], Z. J. Sun[1], X. Tang[1], N. Tao[16], Y. R. Tian[14], G. L. Tong[1], G. S. Varner[15], D. Y. Wang[1], J. Z. Wang[1], L. Wang[1], L. S. Wang[1], M. Wang[1], Meng Wang[1], P. Wang[1], P. L. Wang[1], S. Z. Wang[1], W. F. Wang[1], Y. F. Wang[1], Zhe Wang[1], Z. Wang[1], Zheng Wang[1], Z. Y. Wang[1], C. L. Wei[1], N. Wu[1], Y. M. Wu[1], X. M. Xia[1], X. X. Xie[1], B. Xin[7], G. F. Xu[1], H. Xu[1], Y. Xu[1], S. T. Xue[1], M. L. Yan[16], W. B. Yan[1], F. Yang[9], H. X. Yang[14], J. Yang[16], S. D. Yang[1], Y. X. Yang[3], L. H. Yi[6], Z. Y. Yi[1], M. Ye[1], M. H. Ye[2], Y. X. Ye[16], C. S. Yu[1], G. W. Yu[1], C. Z. Yuan[1], J. M. Yuan[1], Y. Yuan[1], Q. Yue[1], S. L. Zang[1], Y. Zeng[6], B. X. Zhang[1], B. Y. Zhang[1], C. C. Zhang[1], D. H. Zhang[1], H. Y. Zhang[1], J. Zhang[1], J. M. Zhang[4], J. Y. Zhang[1], J. W. Zhang[1], L. S. Zhang[1], Q. J. Zhang[1], S. Q. Zhang[1], X. M. Zhang[1], X. Y. Zhang[11], Yiyun Zhang[13], Y. J. Zhang[10], Y. Y. Zhang[1], Z. P. Zhang[16], Z. Q. Zhang[4], D. X. Zhao[1], J. B. Zhao[1], J. W. Zhao[1], P. P. Zhao[1], W. R. Zhao[1], X. J. Zhao[1], Y. B. Zhao[1], Z. G. Zhao[1], H. Q. Zheng[10], J. P. Zheng[1], L. S. Zheng[1], Z. P. Zheng[1], X. C. Zhong[1], B. Q. Zhou[1], G. M. Zhou[1], L. Zhou[1], N. F. Zhou[1], K. J. Zhu[1], Q. M. Zhu[1], Yingchun Zhu[1], Y. C. Zhu[1], Y. S. Zhu[1], Z. A. Zhu[1], B. A. Zhuang[1], B. S. Zou[1].

(BES Collaboration)

[1] Institute of High Energy Physics, Beijing 100039, People's Republic of China

[2] China Center of Advanced Science and Technology,
Beijing 100080, People's Republic of China

[3] Guangxi Normal University, Guilin 541004, People's Republic of China

[4] Henan Normal University, Xinxiang 453002, People's Republic of China

[5] Huazhong Normal University, Wuhan 430079, People's Republic of China

[6] Hunan University, Changsha 410082, People's Republic of China

[7] Liaoning University, Shenyang 110036, People's Republic of China

[8] Nanjing Normal University, Nanjing 210097, People's Republic of China

[9] Nankai University, Tianjin 300071, People's Republic of China

[10] Peking University, Beijing 100871, People's Republic of China

[11] Shandong University, Jinan 250100, People's Republic of China

[12] Shanghai Jiaotong University, Shanghai 200030, People's Republic of China

[13] Sichuan University, Chengdu 610064, People's Republic of China

[14] Tsinghua University, Beijing 100084, People's Republic of China

[15] University of Hawaii, Honolulu, Hawaii 96822

[16] University of Science and Technology of China, Hefei 230026, People's Republic of China

[17] Wuhan University, Wuhan 430072, People's Republic of China

[18] Zhejiang University, Hangzhou 310028, People's Republic of China

(Dated: February 7, 2008)

Abstract

The processes $\psi(2S) \to \gamma\chi_{cJ}$, $\chi_{cJ} \to p\overline{p}$ $(J = 0, 1, 2)$ are studied using a sample of 14×10^6 $\psi(2S)$ decays collected with the Beijing Spectrometer at the Beijing Electron-Positron Collider. Very clear χ_{c0}, χ_{c1} and χ_{c2} signals are observed, and the branching fractions $\mathcal{B}(\chi_{cJ} \to p\overline{p})$ $(J = 0, 1, 2)$ are determined to be $(27.1^{+4.3}_{-3.9} \pm 4.7) \times 10^{-5}$, $(5.7^{+1.7}_{-1.5} \pm 0.9) \times 10^{-5}$, and $(6.5^{+2.4}_{-2.1} \pm 1.0) \times 10^{-5}$, respectively, where the first errors are statistical and the second are systematic.

PACS numbers: 13.25.Gv, 14.40.Gx, 12.38.Qk

I. INTRODUCTION

Hadronic decay rates of P-wave quarkonium states provide good tests of quantum chromodynamics (QCD). The decays $\chi_{cJ} \to p\overline{p}$ have been calculated using different models [1, 2], and recently, the decay branching fractions of $\chi_{cJ} \to$ baryon and anti-baryon pairs were calculated including the contribution of the color-octet fock (COM) states [3]. Using the $\chi_{cJ} \to p\overline{p}$ branching fractions as input to determine the matrix element, the partial widths of $\chi_{cJ} \to \Lambda\overline{\Lambda}$ are predicted to be about half of those of $\chi_{cJ} \to p\overline{p}$, for $J = 1$ and 2. However, recent measurements of $\chi_{cJ} \to \Lambda\overline{\Lambda}$ [4] together with the branching fractions of $\chi_{cJ} \to p\overline{p}$ from $p\overline{p}$ annihilation experiments [5–7] and from a measurement from $\psi(2S)$ decays [8] seem to contradict this prediction. An improved measurement of the $\chi_{cJ} \to p\overline{p}$ branching fraction with the same data sample that was used for $\chi_{cJ} \to \Lambda\overline{\Lambda}$ measurement will yield a more consistent measurement of this fraction.

The measurements of $\mathcal{B}(\chi_{cJ} \to p\overline{p})$ have been performed in e^+e^- collision experiments, where the χ_{cJ} are produced in $\psi(2S)$ radiative decays, and in $p\overline{p}$ annihilation experiments, where χ_{cJ} are formed directly. Although the precision in these experiments is limited, results from $p\overline{p}$ annihilation experiments seem systematically higher than those obtained in $e^+e^- \to \psi(2S)$ experiments, as shown in Table I. This led to a global fit based on results from both e^+e^- and $p\overline{p}$ annihilations [9].

TABLE I: $\mathcal{B}(\chi_{cJ} \to p\overline{p})$ results obtained by different experiments.

Channel	Experimental technique	
	$\psi(2S) \to \gamma\chi_{cJ} \to \gamma p\overline{p}$	$p\overline{p} \to \chi_{cJ} \to \gamma J/\psi$
$\mathcal{B}(\chi_{c0} \to p\overline{p})(\times 10^{-5})$	15.9±4.3±5.3 [8]	48^{+9+21}_{-8-11} [5]
		$41 \pm 3^{+16}_{-9}$ [6]
$\mathcal{B}(\chi_{c1} \to p\overline{p})(\times 10^{-5})$	4.2±2.2±2.8 [8]	7.8±1.0±1.1 [7]
$\mathcal{B}(\chi_{c2} \to p\overline{p})(\times 10^{-5})$	5.8±3.1±3.2 [8]	9.1±0.8±1.4 [7]

The above e^+e^- annihilation results [8] were obtained from a sample of 3.79×10^6 $\psi(2S)$ events collected with the Beijing Spectrometer (BESI) detector [10] at the Beijing Electron-positron Collider (BEPC) storage ring running at the energy of the $\psi(2S)$. Here we report on a result obtained with a sample of $(14 \pm 0.6) \times 10^6$ $\psi(2S)$ events collected with the upgraded

BESII detector [11]. In BESII, a 12-layer vertex chamber (VTC) surrounding the beam pipe provides trigger information. A forty-layer main drift chamber (MDC), located radially outside the VTC, provides trajectory and energy loss (dE/dx) information for charged tracks over 85% of the total solid angle. The momentum resolution is $\sigma_p/p = 0.018\sqrt{1+p^2}$ (p in GeV/c), and the dE/dx resolution for hadron tracks is $\sim 8\%$. An array of 48 scintillation counters surrounding the MDC measures the time-of-flight (TOF) of charged tracks with a resolution of ~ 200 ps for hadrons. Radially outside the TOF system is a 12 radiation length, lead-gas barrel shower counter (BSC). This measures the energies of electrons and photons over $\sim 80\%$ of the total solid angle with an energy resolution of $\sigma_E/E = 21\%/\sqrt{E}$ (E in GeV). Outside of the solenoidal coil, which provides a 0.4 Tesla magnetic field over the tracking volume, is an iron flux return that is instrumented with three double layers of counters that identify muons of momentum greater than 0.5 GeV/c.

A Monte Carlo (MC) simulation is used for the determination of mass resolution and detection efficiency. The angular distribution of $\psi(2S) \to \gamma X$ is simulated assuming a pure E1 transition, namely $1+\cos^2\theta$, $1-\frac{1}{3}\cos^2\theta$, and $1+\frac{1}{13}\cos^2\theta$ for the spin-parity of the resonance X being $J^P = 0^+, 1^+$ and 2^+, respectively, and X decaying to $p\bar{p}$ is simulated according to phase space. A Geant3 based package, SIMBES, is used for the simulation of detector response, where the interactions of the produced particles with the detector material are simulated and detailed consideration of the detector performance (such as dead electronic channels) is included. Reasonable agreement between data and Monte Carlo simulation has been observed in various channels tested, including Bhabha, $e^+e^- \to \mu^+\mu^-$, $J/\psi \to p\overline{p}$, and $\psi(2S) \to \pi^+\pi^- J/\psi, J/\psi \to \ell^+\ell^-$ ($\ell = e$ or μ).

II. EVENT SELECTION

To select $\psi(2S) \to \gamma\chi_{cJ}$, $\chi_{cJ} \to p\overline{p}$ ($J = 0, 1, 2$) candidates, events with at least one photon and two charged tracks are required. A neutral cluster in the BSC is considered to be a photon candidate when the angle between the nearest charged track and the cluster in the xy plane is greater than 15°, the first cell hit is in the beginning 6 radiation lengths, and the angle between the cluster development direction in the BSC and the photon emission direction in xy plane is less than 37°.

A likelihood method is used for discriminating pion, kaon, proton, and antiproton tracks. For each charged track, an estimator is defined as $W^i = \frac{P^i}{\sum_i P^i}$, $P^i = \prod_j P^i_j(x_j)$, where P^i

is the probability under the hypothesis of being type i, $i = \pi$, K, and p or $\bar{p}$, and $P_j^i(x_j)$ is the probability density for the hypothesis of type i, associated with the discriminating variable x_j. Discriminating variables used for each charged track are the time of flight in the TOF and the energy loss of the track in the MDC. By definition, pion, kaon, proton and antiproton tracks have corresponding W^i value near one.

For the decay channel of interest, the candidate events are required to satisfy the following selection criteria:

1. There are two oppositely charged tracks in the MDC with each track having a good helix fit and $|\cos\theta| < 0.75$, where θ is the polar angle of the track;

2. At least one charged track is identified either as a proton or an anti-proton with $W^p > 0.7$ or $W^{\bar{p}} > 0.7$;

3. There is at least one photon candidate. In the case of multiple photon candidates, the one with the largest BSC energy is chosen as the photon radiated from the $\psi(2S)$;

4. The χ^2 probability of the four-constraint kinematic fit is required to be greater than 1%.

Figures 1a and 1b show distributions of W^p and $W^{\bar{p}}$ after all other requirements have been applied. It can be seen that the $W^{p/\bar{p}} > 0.7$ requirement rejects most of the π and K background, while retaining high efficiency.

In order to reduce backgrounds from e^+e^- or $\mu^+\mu^-$ tracks in J/ψ decays ($\psi(2S) \to XJ/\psi$), the BSC energy of the positively charged track (ESC_p) is required to be less than 0.7 GeV, and the two charged tracks must satisfy the muon veto requirement, that $N_p^{hit} + N_{\bar{p}}^{hit} < 6$, where N^{hit} is the number of mu-counter layers with matched hits and ranges from 0 to 3, indicating not a muon (0), a weak (1), medium (2), or strongly (3) identified muon track [12]. Distributions of ESC_p and $N_p^{hit} + N_{\bar{p}}^{hit}$ are shown in Figures 1c and 1d.

After the above selection, the invariant mass of the proton and anti-proton is shown in Fig. 2a, where clear χ_{c0}, χ_{c1} and χ_{c2} signals can be seen. The large peak near the mass of the $\psi(2S)$ is due to $\psi(2S) \to p\overline{p}$ with a fake photon reconstructed.

The same analysis is performed on a MC sample with 14 M inclusive $\psi(2S)$ decays generated with Lundcharm [13]. It is found that the remaining backgrounds are mainly from $\psi(2S) \to \pi^0 p\overline{p}$ with $\pi^0 \to 2\gamma$, and they contribute a smooth part to the $p\overline{p}$ invariant mass distribution.

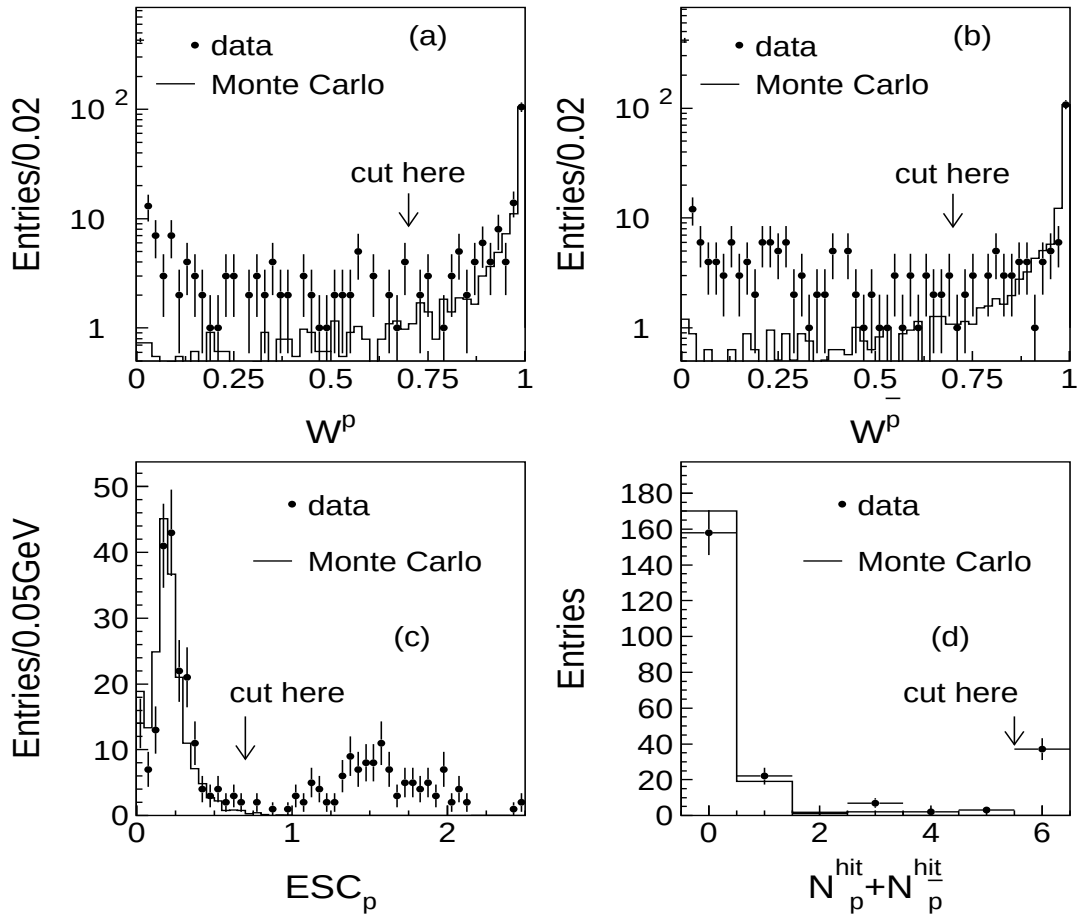

FIG. 1: (a) W^p,(b) $W^{\bar{p}}$,(c) ESC_p, and (d) $N_p^{hit}+N_{\bar{p}}^{hit}$ distributions after all the other requirements have been applied, as described in the text. The histograms are for Monte Carlo simulated $\psi(2S) \to \gamma\chi_{c0}$, $\chi_{c0} \to p\overline{p}$ events and dots with error bars are for data with $p\overline{p}$ invariant mass within the χ_{cJ} signal region. For (a) and (b), data and MC simulation are normalized to the last bin, and for (c) and (d), data and MC simulation are normalized to $ESC_p < 0.7$ and $N_p^{hit} + N_{\bar{p}}^{hit} < 6$, respectively.

III. FIT TO THE $p\bar{p}$ INVARIANT MASS SPECTRUM

The $p\bar{p}$ mass spectrum of the final selected events with $p\bar{p}$ mass between 3.26 and 3.64 GeV/c^2 is fitted with three Breit-Wigner resonances smeared by Gaussian mass resolution functions together with a second order polynomial background using the unbinned maximum likelihood method. In the fit, the mass resolutions are fixed to values from Monte Carlo simulation (6.84, 6.59 and 6.17 MeV/c^2 for χ_{c0}, χ_{c1} and χ_{c2}, respectively), and the widths of χ_{c1} and χ_{c2} are fixed to 0.92 and 2.08 MeV/c^2 coming from the PDG2002 [14]. The fit, shown in Fig. 2a, yields a likelihood probability of 79%, total numbers of events of

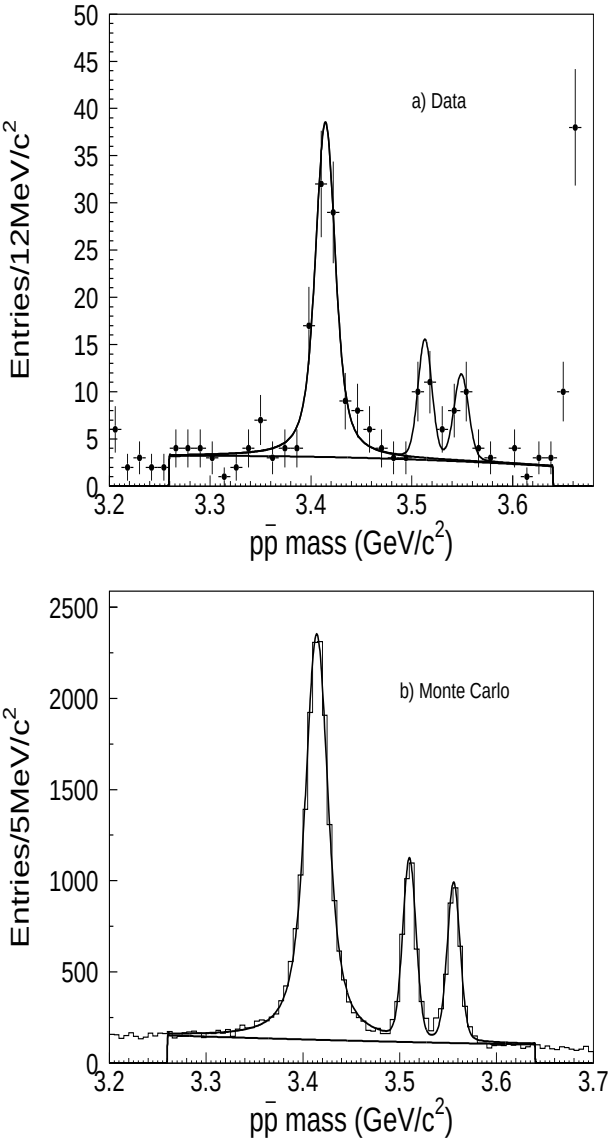

FIG. 2: Breit-Wigner fit to $p\bar{p}$ mass distribution for selected $\psi(2S) \to \gamma p\bar{p}$ events (a) in data and (b) in Monte Carlo simulation, with relative branching fractions fixed to data.

89.5^{+14}_{-13}, $18.2^{+5.5}_{-4.9}$, and $14.3^{+5.2}_{-4.7}$, and statistical significances of 10.6σ, 4.6σ, and 3.7σ for χ_{c0}, χ_{c1} and χ_{c2}, respectively. The fitted masses are 3414.3 ± 1.6, 3513.0 ± 2.1, and $3549.1^{+3.2}_{-3.0}$ MeV/c^2, respectively, and agree well with the world averages [14], and the width of the χ_{c0} is determined to be $12.8^{+5.6}_{-4.5}$ MeV/c^2, in good agreement with results from other experiments [14].

The same fit is applied to the Monte Carlo sample, which is about 180 times larger than the data sample and uses the same relative branching fractions between the three χ_{cJ} states as determined from the data. The background fraction is estimated using the χ_{c0} mass

region for data. The fit yields the efficiencies for each channel as $\varepsilon_{\chi_{c0}} = (27.49 \pm 0.30)\%$, $\varepsilon_{\chi_{c1}} = (27.42 \pm 0.56)\%$, and $\varepsilon_{\chi_{c2}} = (23.26 \pm 0.50)\%$, where the errors are due to the limited statistics of the Monte Carlo samples.

IV. SYSTEMATIC ERRORS

Systematic errors of the measured branching fractions come from the efficiencies of photon identification, particle identification, the kinematic fit, etc.

A. Photon identification

To investigate the systematic error associated with the fake photon misidentification, the fake photon multiplicity distributions and the energy spectra in both data and Monte Carlo sample are checked with $\psi(2S) \to p\overline{p}$ events. In this channel, it is found that the Monte Carlo simulates a little more fake photons than data.

The selection of the photon candidate with the largest BSC energy has an efficiency of $(92.55 \pm 0.52)\%$ for data and $(94.49 \pm 0.22)\%$ for Monte Carlo in $\psi(2S) \to \gamma\chi_{c2} \to \gamma p\overline{p}$, as determined from the comparison of energy distributions between the real photons and the fake ones; the difference is $(2.1 \pm 0.6)\%$. For χ_{c1} and χ_{c0}, the photon is more energetic, so the efficiency of selecting the largest BSC energy cluster is higher. The systematic error on the photon identification is taken as 2.7% for χ_{c2}, as well as for χ_{c0} and χ_{c1}.

B. Photon detection efficiency

The detection efficiency of low energy photons is studied with $J/\psi \to \pi^+\pi^-\pi^0$ events by requiring only one photon in the kinematic fit and examining the detector response in the direction of emission of the second photon. The efficiency from the Monte Carlo simulation agrees with data within 2% in the full energy range. This is taken as the systematic error of the photon detection efficiency.

C. Particle identification

The systematic error from particle identification is studied using p (or $\bar{p}$) samples from $\psi(2S) \to \pi^+\pi^- J/\psi$, $J/\psi \to p\bar{p}$ and $\psi(2S) \to p\overline{p}$. Since only one track is required to be

identified, the efficiency is very high. The correction factors for efficiencies for χ_{c0}, χ_{c1} and χ_{c2} are found to be 1.020±0.006, 1.025±0.006 and 1.028±0.006 respectively.

D. Kinematic fit

The systematic error associated with the kinematic fit is caused by differences between the measurements of the momenta and the error matrices of the track fitting of the charged tracks and the measurement of the energy and direction of the neutral track for the data and the simulation sample. The effect is studied for charged tracks and neutral tracks separately. The systematic error due to the charged tracks was checked using $\psi(2S) \to p\overline{p}$ events, which can be selected easily without using any kinematic fit. By comparing the numbers of the events before and after the kinematic fit, the efficiencies for χ^2 probability $> 1\%$ are measured to be $(85.34 \pm 1.64)\%$ for data and $(88.17 \pm 0.56)\%$ for Monte Carlo simulation, respectively. This results in a correction factor of $(0.968 \pm 0.020)\%$ for the efficiency of this specific channel.

The uncertainty due to the measurement of the neutral track parameters is taken from Ref. [4] based on a study of $\psi(2S) \to \gamma\chi_{cJ}$, $\chi_{cJ} \to \pi^+\pi^- p\overline{p}$. A systematic error of 4.2% is quoted for all the channels.

E. Muon veto and BSC energy requirements

The efficiencies of the muon veto and BSC energy requirements are studied with $\psi(2S) \to p\overline{p}$ events. In order to get a clean sample of $p\overline{p}$ without using these requirements, a four-constraint kinematic fit to $p\overline{p}$ is done, and the χ^2 probability of the fit is required to be greater than 1%. The efficiencies of the muon veto for both data and Monte Carlo simulation are found to be 100%, while those of the BSC energy requirement are $(98.94 \pm 0.40)\%$ and $(99.14 \pm 0.18)\%$ for data and Monte Carlo, respectively, resulting in a difference of $(0.20 \pm 0.44)\%$. This difference together with the error is taken as the systematic error of the BSC energy requirement.

F. Angular distribution

For the radiative decay $\psi(2S) \to \gamma\chi_{cJ}$, the general form of the angular distribution is $W(\cos\theta) = 1 + A\cos^2\theta$, where θ is the angle between the beam direction and the outgoing photon and $|A| \leq 1$ [15]. The value of A can be unambiguously predicted only for spin $J = 0$, where $A = 1$. By comparing the multipole coefficients measured by Crystal Ball [16] with those used under the assumption of pure $E1$ transition, differences of 3.5% and 5.5% are found, which will be taken as systematic errors of the angular distributions for $J = 1$ and 2 respectively.

G. Breit-Wigner fit

To determine the fit systematic errors, different background shapes and fit ranges are used in the fit of the $p\bar{p}$ invariant mass distribution. After changing the background shape from a second order to a first order polynomial and varying the fitting range around the one used in the fit, the uncertainties due to fit are determined to be 11.5%, 8.4% and 7.3% for χ_{c0}, χ_{c1}, and χ_{c2}, respectively.

H. Monte Carlo determined mass resolution

The systematic error due to the use of the MC determined mass resolution is studied with $\psi(2S) \to \pi^+\pi^- J/\psi$, $J/\psi \to p\bar{p}$. The non-Gaussian tails are found to be $(5.3 \pm 4.4)\%$ and $(5.3 \pm 1.9)\%$ for data and Monte Carlo respectively, which indicates good agreement between data and Monte Carlo simulation. The uncertainty of the comparison, 4.8%, is taken as the systematic error due to the MC determined mass resolution.

I. Other systematic errors

The results reported here are based on a data sample corresponding to a total number of $\psi(2S)$ decays, $N_{\psi(2S)}$, of $(14.0 \pm 0.6) \times 10^6$, as determined from inclusive hadronic events [17]. The uncertainty of the number of $\psi(2S)$ events, 4%, is determined from the uncertainty in selecting the inclusive hadrons.

The difference of MDC tracking efficiencies between data and Monte Carlo for p and $\bar{p}$ may cause a systematic error of 1-2% for each track. Here 3% is taken as the systematic error

on the overall tracking efficiency. The trigger efficiency is around 100% with an uncertainty of 0.5%, as estimated from Bhabha and $e^+e^- \to \mu^+\mu^-$ events. The systematic errors on the branching fractions used are obtained from PDG [14] directly.

J. Total systematic error

Table II lists the systematic errors from all sources. Adding all errors in quadrature, the total errors are 17.3%, 15.4% and 15.6% for χ_{c0}, χ_{c1} and χ_{c2}, respectively. The corresponding correction factors (f) for the Monte Carlo simulated efficiencies are 0.987, 0.992, and 0.995.

TABLE II: Summary of systematic errors in percent. Numbers common for all channels are only listed once.

Source	χ_{c0}	χ_{c1}	χ_{c2}
MC statistics	1.1	2.0	2.2
Photon I.D.		2.7	
Photon eff.		2	
4C-fit(neutral)		$\leq$4.2	
4C-fit(charged)		2.0	
Particle I.D.		0.6	
BW fit	11.5	8.4	7.3
Mass resolution		4.8	
BSC energy cut		0.6	
Angular distr.	0	3.5	5.5
Number of $\psi(2S)$		4	
MDC Tracking		3	
Trigger Efficiency		0.5	
$\mathcal{B}(\psi(2S) \to \gamma\chi_{cJ})$	9.2	8.3	8.8
Total Systematic error	17.3	15.4	15.6

V. RESULTS

The branching fraction of $\chi_{cJ} \to p\overline{p}$ is calculated using

$$\mathcal{B}(\chi_{cJ} \to p\bar{p}) = \frac{n^{obs}/(\varepsilon \cdot f)}{N_{\psi(2S)} \cdot B[\psi(2S) \to \gamma\chi_{cJ}]}.$$

Using numbers listed in Table. III, one obtains

$$\begin{aligned}
\mathcal{B}(\chi_{c0} \to p\overline{p}) &= (27.1^{+4.3}_{-3.9} \pm 4.7) \times 10^{-5}, \\
\mathcal{B}(\chi_{c1} \to p\overline{p}) &= (5.7^{+1.7}_{-1.5} \pm 0.9) \times 10^{-5}, \\
\mathcal{B}(\chi_{c2} \to p\overline{p}) &= (6.5^{+2.4}_{-2.1} \pm 1.0) \times 10^{-5},
\end{aligned}$$

where the first errors are statistical and the second are systematic. The measured branching fractions agree with corresponding world averages within errors [14].

TABLE III: Numbers used in branching fraction calculation and the final results.

quantity	χ_{c0}	χ_{c1}	χ_{c2}
n^{obs}	89.5^{+14}_{-13}	$18.2^{+5.5}_{-4.9}$	$14.3^{+5.2}_{-4.7}$
ε (%)	27.49±0.30	27.42±0.56	23.26±0.50
f	0.987	0.992	0.995
$N_{\psi(2S)}(10^6)$		14	
$\mathcal{B}[\psi(2S) \to \gamma\chi_{cJ}](\%)$	(8.7±0.8)%	(8.4±0.7)%	(6.8±0.6)%
$\mathcal{B}(\chi_{cJ} \to p\overline{p})$ (10^{-5})	$27.1^{+4.3}_{-3.9} \pm 4.7$	$5.7^{+1.7}_{-1.5} \pm 0.9$	$6.5^{+2.4}_{-2.1} \pm 1.0$
$R_{\mathcal{B}}$	1.73 ± 0.63	4.56 ± 2.34	5.08 ± 3.08

The relative branching fraction of $\chi_{cJ} \to \Lambda\overline{\Lambda}$ to $\chi_{cJ} \to p\overline{p}$ is found with the following formula:

$$R_{\mathcal{B}} = \frac{n^{obs}_{\Lambda\overline{\Lambda}}/[\varepsilon_{\Lambda\overline{\Lambda}} \cdot \mathcal{B}(\Lambda \to \pi^- p)^2]}{n^{obs}_{p\overline{p}}/\varepsilon_{p\overline{p}}}.$$

These results are also shown in Table III, by using the numbers in Table III of this paper and those in Table II of Ref. [4], with the common errors in $\mathcal{B}(\chi_{cJ} \to \Lambda\overline{\Lambda})$ and $\mathcal{B}(\chi_{cJ} \to p\overline{p})$ canceled out. The measurements confirm the enhancement of $\chi_{cJ} \to \Lambda\overline{\Lambda}$ relative to $\chi_{cJ} \to p\overline{p}$, as compared with the COM calculation [3].

The actual measured quantities in this analysis is the branching fractions of $\psi(2S) \to \gamma\chi_{cJ} \to \gamma p\overline{p}$, with

$$\begin{aligned}\mathcal{B}[\psi(2S) \to \gamma\chi_{cJ} \to \gamma p\overline{p}] &= \mathcal{B}[\psi(2S) \to \gamma\chi_{cJ}] \cdot \mathcal{B}(\chi_{cJ} \to p\overline{p}) \\ &= \frac{n^{obs}/(\varepsilon \cdot f)}{N_{\psi(2S)}},\end{aligned}$$

using numbers in Table III, the results are

$$\begin{aligned}\mathcal{B}[\psi(2S) \to \gamma\chi_{c0} \to \gamma p\overline{p}] &= (23.6^{+3.7}_{-3.4} \pm 3.4) \times 10^{-6}, \\ \mathcal{B}[\psi(2S) \to \gamma\chi_{c1} \to \gamma p\overline{p}] &= (4.8^{+1.4}_{-1.3} \pm 0.6) \times 10^{-6}, \\ \mathcal{B}[\psi(2S) \to \gamma\chi_{c2} \to \gamma p\overline{p}] &= (4.4^{+1.6}_{-1.4} \pm 0.6) \times 10^{-6}.\end{aligned}$$

VI. SUMMARY

Decays $\chi_{cJ} \to p\overline{p}$ are observed using the BESII sample of 14 million $\psi(2S)$ events, and the corresponding branching fractions are determined. The measured values agree with previous experiments within errors [5–8]. The measurements confirm the enhancement of $\chi_{cJ} \to \Lambda\overline{\Lambda}$ relative to $\chi_{cJ} \to p\overline{p}$, as compared with the COM calculation [3].

Acknowledgments

The BES collaboration thanks the staff of the BEPC for their hard efforts. This work is supported in part by the National Natural Science Foundation of China under contracts Nos. 19991480, 10225524, 10225525, the Chinese Academy of Sciences under contract No. KJ 95T-03, the 100 Talents Program of CAS under Contract Nos. U-11, U-24, U-25, and the Knowledge Innovation Project of CAS under Contract Nos. U-602, U-34(IHEP); by the National Natural Science Foundation of China under Contract No. 10175060 (USTC); and by the U.S. Department of Energy under Contract No. DE-FG03-94ER40833 (U Hawaii).

[1] M. Anselmino, R. Cancelliere, and F. Murgia, Phys. Rev. **D46**, 5049 (1992).

[2] M. Anselmino, F. Caruso, and S. Forte, Phys. Rev. **D44**, 1438 (1991);
M. Anselmino and F. Murgia, Z. Phys. **C58**, 429 (1993).

[3] S. M. H. Wong, Eur. Phys. J. **C14**, 643 (2000).

[4] J. Z. Bai. *et al.* (BES Collab.), Phys. Rev. **D67**, 112001 (2003).

[5] M. Ambrogiani *et al.* (E835 Collab.), Phys. Rev. Lett. **83**, 2902 (1999).

[6] S. Bagnasco *et al.* (E835 Collab.), Phys. Lett. **B533**, 237 (2002).

[7] T. A. Armstrong *et al.* (E760 Collab.), Nucl. Phys. **B373**, 35 (1992).

[8] J. Z. Bai *et al.* (BES Collab.), Phys. Rev. Lett. **81**, 3091 (1998).

[9] C. Patrignani, Phys. Rev. **D64**, 034017 (2001).

[10] J. Z. Bai. *et al.* (BES Collab.), Nucl. Instr. Meth. **A344**, 319 (1994).

[11] J. Z. Bai. *et al.* (BES Collab.), Nucl. Instr. Meth. **A458**, 627 (2001).

[12] J. Z. Bai. *et al.* (BES Collab.), HEP&NP **20**, 97 (1996) (in Chinese).

[13] J. C. Chen *et al.*, Phys. Rev. **D62**, 034003 (2000).

[14] K. Hagiwara *et al.* (Particle Data Group), Phys. Rev. **D66**, 010001 (2002).

[15] G. Karl, S. Meshkov and J. Rosner, Phys. Rev. **D13**, 1203 (1976); W. Tanenbaum *et al.*, Phys. Rev. **D17**, 1731 (1978); P. K. Kabir and A. J. G. Hey, Phys. Rev. **D13**, 3161 (1976).

[16] M. Oreglia *et al.* (Crystal Ball Collab.), Phys. Rev. **D25**, 2259 (1982).

[17] J. Z. Bai. *et al.* (BES Collab.), Phys. Lett. **B550**, 24 (2002).